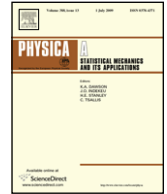




Contents lists available at ScienceDirect

Physica A

journal homepage: www.elsevier.com/locate/physa

Scattering in thick multifractal clouds, Part I: Overview and single scattering

B.P. Watson^a, S. Lovejoy^{b,*}, Y. Grosdidier^b, D. Schertzer^c

^a Department of Physics, St. Lawrence University, Canton, NY 13617, USA

^b Department of Physics, McGill University, 3600 University Street, Montreal, Que., Canada

^c CERERE, Ecole Nationale des Ponts et Chaussées, 6-8, avenue Blaise Pascal, Cité Descartes, 77455 MARNE-LA-VALLEE Cedex, France

ARTICLE INFO

Article history:

Received 1 October 2008

Received in revised form 1 May 2009

Available online xxxx

Keywords:

Light scattering

Multifractal

Clouds

Turbulence

Transport in disordered media

ABSTRACT

Over the last twenty years, many studies have been made of radiative transfer in scaling cloud fields, the vast majority of which have been limited to numerical studies in clouds with relatively small optical thickness. An exception to this was the development of a formalism for treating single scattering in optically thick but conservative multifractal clouds without significant holes. In part I of this paper we show how these results can be extended to general “universal” multifractal clouds dominated by low density “Lévy holes”. In part II, we demonstrate how the analytic single scattering results can be generalized to multiple scattering including the case of very thick clouds as well as to realistic nonconservative clouds.

© 2009 Elsevier B.V. All rights reserved.

1. Introduction

1.1. Overview

Clouds – both meteorological and astrophysical – and their associated radiation fields are highly variable over huge ranges of space–time scales. An understanding of both the variability and the inter-relation between the two fields is of fundamental importance in meteorology, climatology, and astrophysics. The relation between radiation fields and the associated scatter density fields is also a challenging problem in the physics of disordered media (sporting several novel statistical features). This problem generally arises in systems with temporal and spatial variability originating in turbulent or turbulent-like phenomena: it is ubiquitous.

Turbulent atmospheric or magneto-turbulent astrophysical dynamics span huge ranges of scale, the natural framework is scaling fields, *i.e.*, multifractals. Indeed, in the atmosphere direct analyses of measurements of visible, near infra red, thermal infra red, passive and active microwave wavelengths (11 bands in all) using 1000 orbits of satellite data spanning the scales of 20,000 to 8 km has recently shown that the radiance fields are multifractal with deviations of the order $\pm 0.5\%$ (short and long waves), $\pm 1.5\%$ to $\pm 4.6\%$ (passive and active microwaves respectively) are scaling over the range from 5000 km on down [1]. These findings greatly improve on earlier indirect and more limited results [2,3]. In this framework, the various cloud morphologies and types are simply manifestations of anisotropic (but still scaling) multifractal generating mechanisms. In astrophysical systems, scaling has been observed from planetary and stellar scales, up to interstellar and even galactic scales (e.g. Refs. [4–9] and references therein).

* Corresponding address: Department of Physics, McGill University, 3600 University Street, Montreal, Que. H2A 2T8, Canada. Tel.: +1 514 398 6537; fax: +1 514 398 8434.

E-mail address: lovejoy@physics.mcgill.ca (S. Lovejoy).

Similarly, many astrophysical plasmas appear to be manifestations of magneto-hydrodynamical turbulence and have been modeled by turbulent fragmentation processes. Many studies were indeed devoted to monofractal characterizations of several astrophysical density or velocity fields (e.g. Refs. [10–17] and references therein). More recently, the multifractal nature of intermittency has been recognized because intermittency affects many chemical reactions and, more generally, because it has a profound impact on structure formation (e.g. Refs. [9,17] and references therein). Hence, as in terrestrial clouds, one is led to adopt the multifractal approach in order to realistically describe astrophysical cloud morphologies and dynamics. Finally, there is also a strong need for quantitative results of radiative transport in astrophysical plasmas since most (if not all) of the information obtained from distant astrophysical sources is in the form of electromagnetic radiation. Note however that the magneto-hydrodynamical turbulence observed in some nebulae or giant molecular clouds (apparently supersonic) are different from atmospheric turbulence [9,13]. The latter is notably distinguished by its vertical stratification which is nevertheless scaling [18–25]. The large compressibility of the nebular gases and the possible multiplicity of turbulence energy sources are likely the main explanations for that difference.

In this paper, we focus on the theoretically well-posed statistical physics problem of radiative transport in multifractal media. There are two parts to the problem each with corresponding model choices. The first is for the medium (referred to as “cloud”), the second is for the transfer. For simplicity, we will limit our attention to isotropic (self-similar) multifractals, and to multifractals with stable, attractive generators: the “universal multifractals”. As for the choice of transport model, we opt for the traditional radiative transfer equation although for some calculations we make a special choice of scattering phase function such that scattering only occurs through a discrete set of angles. This makes the numerics particularly exact [26–28] without modifying the basic statistical properties of the transport (the scaling exponents). The slightly simpler transport problem of diffusion on multifractals [29–33] is itself quite interesting, but (except in 1-D [32,34]) is not in the same universality class as radiative transport [26]. It could be mentioned that much of the work on transport in scaling media has focused on binary systems in which the medium is modeled as a geometric set of points (e.g. the problem of electrical conduction in a conducting percolating system, see the reviews [35,36]); the corresponding geometric fractal sets are simpler than the multifractal measures relevant to turbulence.

1.2. External horizontal variability, and fractal models

The theory of radiative transfer in plane parallel horizontally homogeneous (1-D) media is elegant and general [37]. However, when we turn to horizontally inhomogeneous media there is no consensus on the appropriate model, nor is the transport problem analytically tractable. For these reasons the use of 1-D models has long dominated the field: in fact, the effect of horizontal variability was both underestimated and neglected. Up until the 1990’s, on the occasions where horizontal inhomogeneity was considered at all, it was usually reduced to the inhomogeneity of the external cloud/medium boundary (e.g. cubes, spheres, cylinders [38–40]) with the internal cloud and radiance fields still being considered smoothly varying if not completely homogeneous. When stronger internal horizontal inhomogeneity was considered it was typically confined to narrow ranges of scale so that various transfer approximations could be justified, see Refs. [41,42]. When the problem of transfer in inhomogeneous media finally came to the fore, the mainstream approaches were heavily technical, (see Gabriel et al. [43] for a review) with emphasis on intercomparisons of general purpose numerical radiative transfer codes (see e.g. the C^3 initiative [44]) and see, e.g., the application to huge Large Eddy Simulation cloud models [45]. At a more theoretical level, the general problem of the consequences of small scale cloud variability on the large scale radiation field has been considered using wavelets [46,47] but has only been applied to numerical modeling. As a consequence, these “3D radiative transfer approaches” have generally shed little light on the scale by scale statistical relations between cloud and radiation fields in realistic scaling clouds (see the collection [48] for more of this numerically intensive classical approach). Overall, there has been far too much emphasis on techniques and applications with little regard for understanding the basic scientific issues.

Motivated by the explosion of interest in scaling systems and the realization that many geophysical systems (including clouds) were scaling over large ranges, the first studies of radiative transport on extremely variable (but mono fractal) systems appeared in which the cloud was modeled as a fractal set but with constant density on the support (e.g. Refs. [26–28,49–54]). These works used various essentially academic fractal models and focused on the (spatial) mean (i.e., bulk) transmission and reflectance. They clearly showed that (i) fractality generally leads to non-classical (“anomalous”) thick cloud scaling exponents, (ii) the latter were strongly dependent on the type of scaling of the medium, and (iii) the exponents are generally independent of the phase function [26].

By the 1990’s, it was clear that scaling generically leads to multifractal fields and that clouds were – as expected for turbulent fields – more nearly multi- rather than mono- fractal so that one must consider a whole range of cloud densities each characterized by a different fractal dimension [55,56]. This pointed to the importance of understanding transport in the more realistic multifractal systems. Since the generic multifractal process is the multiplicative cascade, this led to transport studies on cascade based cloud models. The two classes of cloud model which have been used for this purpose are the fractionally integrated flux model (FIF) [57] and the bounded cascade model [54]. In the FIF model, a multiplicative cascade generates a (scale by scale) conservative multifractal (for example, the energy flux to smaller scales), then a fractional integration (i.e. a power law filtering) is used to model the turbulent velocity or passive scalar density field; the details are recalled in Section 2. This model attempts to reproduce the phenomenology and scaling of passive scalar turbulence, in particular it yields statistics following the intermittent generalization of the classical Corrsin–Obukhov law of passive

scalar advection. Not only are the second order statistics correct (e.g. the spectrum is of the roughly $k^{-5/3}$) form, but the intermittency corrections/exponents (the statistics of orders other than second) can be made very close to those of real clouds. In contrast in the bounded cascade model, there is no conserved flux, the velocity or density fields are directly modeled with multiplicative cascades which are strongly “bounded” in order to obtain the observed second order passive scalar statistics (spectra). The bounding is effected by progressively and rapidly weakening the cascade at each step. As pointed out [3], this scale by scale attenuation essentially kills off the intermittency so that the resulting field has the same scaling exponents as a truncated (non-intermittent, additive) gaussian process. Studies of radiative transport on the latter have unsurprisingly concluded that the effect of the horizontal cloud heterogeneity on the radiative transfer is small [54]. Recently some proponents of the bounded cascade [58] have admitted that the FIF is indeed more realistic than the bounded cascade – perhaps signaling renewed interest in models with stronger, more realistic variability.

Finally, it is worth mentioning a related approach proposed by Davis et al. [59] to phenomenologically account for the cloud variability. These authors proposed replacing the standard exponential transmission (Green’s) function by a power law corresponding to a Lévy flight model for photon paths. The justification is that cloud “holes” give rise to occasionally very long photon paths. While this model is interesting, it is not clear which – if any – cloud processes would give rise to Lévy flights. It is interesting to note that the multifractal cloud models discussed here have Lévy generators for the cloud density field, and do indeed give rise to quite long tailed distributions of photon path lengths – but they turn out not to be truly “fat-tailed” (algebraic) such as in Lévy distributions. Although photon paths do exhibit clustering and other features of the Lévy walks (see Figs. 4 and 5), they in fact have finite variances. In addition, the Lévy flights correspond to “superdiffusion” in which, after N scatters photons travel a distance N^{1/D_F} with $D_F < 2$ whereas – due to the “trapping” of photons in dense regions – we find $D_F > 2$ i.e. “subdiffusion” corresponding to a different phenomenology.

1.3. Transport in multifractal media

To date nearly all numerical studies of radiative transport in multifractal media have used the special Discrete Angle (DA) phase functions mentioned above and described in detail in Section 4 (an exception is Evans [60] who used a backward Monte Carlo technique and approximations valid for optically thin clouds). In addition, for reasons of convenience, they have concentrated almost exclusively on two dimensional systems (see however Refs. [61–64]) with periodic horizontal boundary conditions and vertically incident radiation. Early studies were primarily numerical [65,66] and aimed at demonstrating the potentially large effect of multifractal heterogeneity on the spatially averaged (“bulk effect”) transport. For example, the latter papers found that for a cloud with strong intermittency characterized by the codimension of the mean $C_1 = 1/2$ (see Section 2; this is very large compared to realistic cloud values $C_1 \approx 0.1$), and mean optical thickness 100, that the mean transmission is increased by a factor of 3 with respect to the homogeneous counterpart. Similarly, Borde and Isaka [64] numerically studied the statistical variation of mean cloud transmittances concentrating on the phase function and other parameters thought to be meteorologically most realistic. Since their clouds had relatively small effective optical thicknesses, the effect of the multifractality was not so large (the transfer problem becomes linear in the optically thin limit so that heterogeneity is no longer important).

More recent approaches have attempted to obtain more theoretical insight into the relation between the multifractal cloud and associated radiation fields. Based on the radiative transfer Green’s function, Naud et al. [67] have argued that with respect to the cloud, the radiation is a kind of integration (presumably of fractional order). These authors showed that since multifractal fields are superpositions of singularities of all orders, above a given critical value the effect of this integration is simply to shift all the singularities (below this value, they are smoothed out). Developing this idea further with the help of a novel statistical closure technique, Schertzer et al. [68] showed that the transfer is indeed an integral over the cloud but over a generally fractal flux tube. This gives a multifractal generalization of the Independent Pixel Approximation (IPA) often used to interpret satellite cloud radiances. Unfortunately this insight has not been developed further.

In this paper, we primarily follow an approach based on the classical order of scattering method for solving the radiative transfer equation (the basis of the Monte Carlo solution method). The starting point is the exact calculation of single scattering statistics in multifractal clouds obtained by averaging the single scatter transmission function over the cloud statistics [34], a “mean field” type of result. This is used to justify a renormalization of the cloud, i.e. to replace the heterogeneous multifractal cloud by an “equivalent” thinner, but homogeneous cloud. In the special multifractals with analytic statistical exponents $K(q)$, (see below) considered in Ref. [66] this theoretically derived renormalization was shown to reproduce the numerical results and was fairly accurate even in optically thick clouds with high degrees of multiple scattering.

While these results were promising, they could not be directly applied to realistic clouds for several reasons. The first is that the cloud was assumed to be a conserved multifractal (a scale by scale energy or passive scalar variance flux). This means that the density fields are much rougher than those of (non-conserved) realistic clouds. The second is that realistic clouds have low density regions (“Lévy holes”) which occur so frequently that their statistics are qualitatively different: negative moments of the cloud density fluctuations diverge and the moment scaling function $K(q)$ is not analytic at the origin. This latter property is the source of serious (and interesting) technical difficulties discussed below. Both cloud density and radiation observations [3,69,70] show that they are indeed nonconservative and furthermore, they quantify the degree of nonanalyticity of $K(q)$. In this paper, we generalize these earlier results obtaining renormalization methods for realistic multifractal exponent

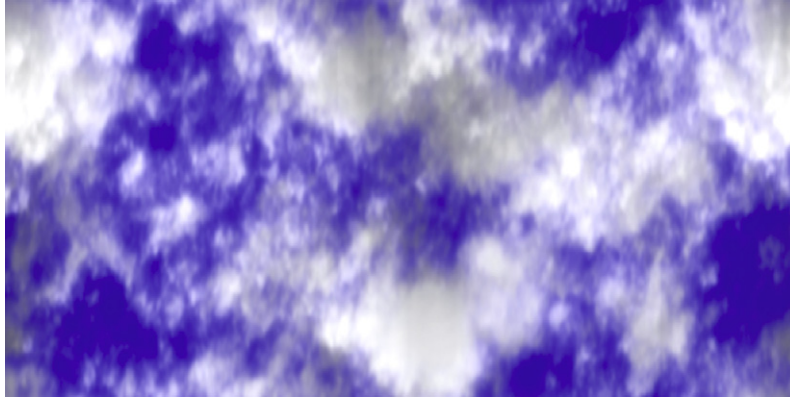


Fig. 1a. This figure shows a top view of a numerical simulation of the radiation field of 512×256 FIF multifractal cloud, 128 pixels thick with horizontal exponents $H = 1/3$, $C_1 = 0.1$ and with $\alpha = 1.75$. The vertical is stratified so that H, C_1 in the vertical direction are a factor $H_2 = 9/5$ larger (see Ref. [19]). The cloud is viewed looking down on the top with the sun at a 45° angle to the right. Only single scattering was used for this rendition. High radiance regions appear white, low radiance regions appear black. Note the presence of very large low valued density regions which are of fundamental importance because they are relatively optically transparent. For more multifractal cloud and radiation simulations, see the site: <http://www.physics.mcgill.ca/~gang/multifrac/index.htm>.

functions. We then consider the extension from single to multiple scattering. The key aspect remaining to be treated for realistic multifractal clouds is the effect of scaling vertical anisotropy responsible for the vertical stratification see Refs. [19–21] for recent empirical results.

This paper is structured as follows. In Section 2 we review the basic multifractal formalism and scale by scale statistics, and review relevant existing results of radiative transfer on multifractal clouds deriving fairly general relations between cloud and (single scattering) radiation statistics (via their corresponding exponents) for clouds with analytic moment scaling exponents $K(q)$. In Section 3, we extend these results for nonanalytic $K(q)$ believed to be necessary for real clouds showing that because of the frequent large “holes” there are asymptotically dominant (thick cloud) corrections to the previous results. In Section 4 we conclude. In part II, we consider multiple scattering using both Monte Carlo and numerical solutions to the transfer equation showing how the single scattering result can be (approximately) extended to multiple scattering. In hindsight, it is surprising that much of the single scattering formalism developed in part I carries over to multiple scattering.

2. Single scattering in multifractal clouds

2.1. Multifractal cloud densities

In this section we derive the single scattering statistics through a multifractal cloud; the presentation is somewhat simplified and improved with respect to that of Ref. [34] largely thanks to the systematic use of the Mellin transform.

As a model we take a cloud with a multifractal density field $\rho(\underline{x})$ (nondimensionalized with $\langle \rho \rangle = 1$, $\underline{x} = (x, y, z)$) where x, y, z are the spatial coordinates nondimensionalized by the outer scale so that the cloud is effectively defined over the unit square (unit cube in 3D). Following basic turbulence phenomenology, we first define a (scale by scale) conservative multifractal φ_λ with the following ensemble averaged moments at scale ratio $\lambda > 1$ which is the ratio of the largest cloud scale (unity), to the scale of observation:

$$\langle \varphi_\lambda^q \rangle = \lambda^{K(q)} \quad (1)$$

where $K(q)$ is the (convex) moment scaling function.

According to the usual turbulence phenomenology, the directly observable cloud density fluctuation is related to the conserved flux φ_λ by:

$$\rho_\lambda = \varphi_\lambda \lambda^{-H} \quad (2)$$

ρ_λ is the fluctuation over scale ratio λ (i.e. nondimensional distance λ^{-1}). For example, according to Corrsin–Obukov [71,72] theory of passive scalars, $\varphi = \chi^{3/2} \varepsilon^{-1/2}$, where χ is the passive scalar variance flux, ε is the energy flux and $H = 1/3$. In the horizontal, Refs. [19,73] have shown empirically that this is close to the observations. Eq. (2) is essentially the result of dimensional analysis, the linear scaling factor λ^{-H} is interpreted statistically. In order to make a stochastic model of a field with the scaling statistics indicated in Eq. (2), the simplest procedure is to use the fractionally integrated flux (FIF) model [57], in which it is modeled as a fractional integration of order H . See Figs. 1a and 1b for representative 3D simulations rendered using single scattering radiative transfer and Figs. 1a and 1b of Part II of this paper for isotropic 2D simulations with false colors comparing the effects of $H = 0, H = 1/3$.



Fig. 1b. Radiances from the same cloud as in Fig. 1a except that it is a side view. The cloud is progressively horizontally stratified at scales greater than 32 pixels (it is progressively vertical stratified as smaller scales).

Mathematically, $K(q)$ could be practically any convex function, so that multifractal modeling and analysis would require an unknown function, the equivalent of an infinite number of parameters. Fortunately, multifractal processes possess stable and attractive generators Γ_λ :

$$\begin{aligned} \Gamma_\lambda &= n_D C_1^{1/\alpha} \gamma_\alpha * |x|^{-D/\alpha} \\ \varphi_\lambda &= e^{\Gamma_\lambda} \end{aligned} \quad (3)$$

where γ_α is a unit, independent and identically distributed Lévy noise “subgenerator” (of index α) and where “*” is the convolution operator [57] and D is the dimension of space. C_1 is the codimension of the mean and determines the mean level of intermittency; the normalization constant n_D depends on the dimension of space and possible scaling anisotropy and will not concern us here. The corresponding conservative “universal” multifractal process φ_λ is then characterized by only two parameters, α and C_1 :

$$K(q) = \frac{C_1}{\alpha - 1} (q^\alpha - q) \quad (4)$$

where $0 \leq \alpha \leq 2$ is the Lévy index of the generator ($= \log \varphi_\lambda$; this is a Lévy process) and C_1 is the codimension of the singularities which give the dominant contribution to the mean of the process (recall that the codimension of a set is the difference between the dimension of space in which the process is embedded and the dimension of that given set). When $\alpha = 2$, γ_α is a gaussian white noise and the “bare” φ_λ (i.e. the process cut-off at the finite resolution $1/\lambda$) is just a log-normal process. In this case, $K(q)$ is quadratic, hence analytic. However, when $\alpha < 2$, the Lévy generator with its long algebraic tail qualitatively changes the statistics and the phenomenology. In order for the moments $q > 0$ of φ_λ to converge; it must be an asymmetrical “extremal Lévy” (i.e. with the extreme algebraic Lévy fluctuations only on the negative side). The negative moments ($\langle \varphi_\lambda^q \rangle$, $q < 0$) diverge due to the frequent large negative values of Γ . This leads to the presence of “Lévy holes” (see Fig. 1a of Part II) which are (possibly) large low valued density regions; for radiative transfer, they play a fundamental role since they are relatively optically transparent.

The above equations define the statistics of ρ via the moments; they can also be defined via their probability distributions:

$$\Pr(\varphi_\lambda > s) \sim \lambda^{-c(\gamma)}; \quad s = \lambda^\gamma \quad (5)$$

where “ \sim ” indicates equality to within slowly varying (e.g. logarithmic) factors. The moments and the probability densities are related by a Mellin transformation [74] see Eq. (19)); this reduces to a Legendre transformation [75] for the exponents:

$$\begin{aligned} c(\gamma) &= \max_q (q\gamma - K(q)) \\ K(q) &= \max_q (q\gamma - c(\gamma)). \end{aligned} \quad (6)$$

Eqs. (6) imply one to one relations between moments and singularities:

$$\gamma = K'(q); \quad q = c'(\gamma). \quad (7)$$

For universal multifractals (i.e. with $K(q)$ given by Eq. (4)),

$$\begin{aligned} c(\gamma) &= C_1 \left(\frac{\gamma}{C_1 \alpha'} + \frac{1}{\alpha} \right)^{\alpha'} \\ &= C_1 \alpha^{-\alpha'} \left(1 - \frac{\gamma}{\gamma_0} \right)^{\alpha'}; \quad 0 \leq \alpha < 1, 1 < \alpha \leq 2 \end{aligned} \quad (8)$$

where: $\frac{1}{\alpha} + \frac{1}{\alpha'} = 1$ and $\gamma_0 = -C_1 \frac{\alpha'}{\alpha} = -\frac{C_1}{\alpha-1}$. It is valid for $\gamma > \gamma_0$ for $1 < \alpha < 2$ ($=0$ otherwise) and for $\gamma < \gamma_0$ for $0 \leq \alpha < 1$ ($=\infty$ otherwise). For $\alpha = 2$ the above is valid for all γ . From Eq. (8) we see that for $1 < \alpha \leq 2$, γ_0 is the largest space filling singularity (the codimension being 0). In addition, since for $1 < \alpha < 2$, $c'(\gamma_0) = 0$, we see that it is also the most probable and gives the dominant contribution to the zeroth order ($q = 0$) cloud density moment. The low order singularities $\gamma < \gamma_0$ corresponding to space filling ($c(\gamma) = 0$) behavior have sub-exponential probabilities: $p(\gamma) \approx |\gamma|^{-\alpha-1}$

(for $\gamma \ll \gamma_0$) corresponding to $p(\varphi) \approx |\log \varphi|^{-\alpha-1}$ as $\varphi \rightarrow 0$. This log divergence of the probability density for small φ leads to frequent low φ regions; the ‘‘Levy holes’’.

Although real cloud fields are not conservative with H empirically close to the theoretical (Corrsin–Obukhov) passive scalar value $1/3$ (rather than zero), in the first part of this paper, and for the sake of simplicity, we restrict ourselves to the conservative case with universal multifractal parameters $H = 0$, $1 < \alpha \leq 2$, and $0 \leq C_1 \leq 2$ (for the 2-D case). Whenever formulae are explicitly evaluated or graphical results displayed, we choose the values $\alpha = 1.75$ and $C_1 = 0.1$, which approximate the parameters found in real clouds [2,76].

In the following, we nondimensionalize distances by the overall cloud size so that ρ_λ is the mean cloud density over the entire cloud. Also, we nondimensionalize the cloud density by a climatological mean value so that $\langle \rho_1 \rangle = 1$. In the theoretical development Section 3 we consider the pure multiplicative process $H = 0$ so that we have $\langle \rho_\lambda \rangle = 1$ (at any scale). Also in this case:

$$\langle \rho_\lambda^q \rangle = \lambda^{K(q)} = \int p_\lambda(\gamma) \lambda^{\gamma q} d\gamma \tag{9}$$

where the probability density $p_\lambda(\gamma)$ is (to within slowly varying factors) $= \lambda^{-c(\gamma)}$ (c.f. Eq. (5) with φ_λ replaced by ρ_λ).

The codimension multifractal formalism presented above was developed to deal with stochastic multifractal fields defined on infinite dimensional probability spaces. At about the same time, a dimension multifractal formalism was developed for handling multifractals on low dimensional phase spaces of (deterministic) chaotic systems [77]. The relation between the two is:

$$\begin{aligned} f(\alpha) &= D - c(\gamma); & \alpha &= D - \gamma \\ \tau(q) &= (q - 1)D - K(q). \end{aligned}$$

Whereas γ is the order of singularity of the multifractal density (φ) the dimension formalism α (not to be confused with the Levy index used here) is the scaling exponent of the corresponding multifractal measure (the integral over a space dimension D of φ). Similarly whereas c is the statistical codimension characterizing the scaling of the probability densities, f is the geometrical fractal dimension of the set of points with corresponding exponent α (or γ). Whenever $c < D$, the c is also equal to the corresponding geometric codimension, however, in general rare events exist for which $c > D$ so that f would have negative values corresponding to impossible negative dimensions. In the codimension formalism, taking $D \rightarrow \infty$ (e.g. for probability spaces) poses no difficulty whereas the dimension formalism quantities diverge. Similar remarks hold for the moment exponents $\tau(q)$ and $K(q)$. More recently, the Multifractal Detrended Fluctuation Analysis method (MDFA) has been developed for multifractal analysis, introducing further exponents (note that the MDFA is not a multifractal formalism per se, it is an analysis technique). To see the relationship between the MDFA exponents and those of the codimension formalism, take the ensemble average of the q th power of both sides of Eq. (2) then the fluctuation exponent:

$$\langle \rho_\lambda^q \rangle = \lambda^{-\xi(q)}; \quad \xi(q) = qH - K(q).$$

Then if we analyze the field ρ_λ with the n th order MDFA technique, then one obtains the exponent $h(q)$ [78]:

$$h(q) = 1 + \xi(q)/q; \quad -1 < H < n.$$

The advantage of this notation is that if there is no intermittency ($K(q) = 0$), then $h = 1 + H$, which is convenient. Caution must be used, however, since – due to the q in the denominator – $h(q)$ can diverge, whereas $\xi(q)$ and $K(q)$ remain finite (for example, if the MDFA is applied to monofractal ‘‘beta model’’ cascade processes or indeed to any universal multifractal with $\alpha < 1$, then $h(q)$ will diverge as $q \rightarrow 0$). The reason that h exceeds H by 1 is because the MDFA analyses the integral of a series so that the total order of integration becomes $1 + H$. Due to this extra 1-D integration, the MDFA must be applied to 1-D sections of two or higher dimensional fields.

2.2. Cloud radiative properties

The extinction parameter κ is the sum of the scattering plus absorption cross-section per unit mass of scattering media; it has dimensions of inverse distance. It characterizes the strength of the matter-radiation coupling; the optical density $\kappa \rho$. For simplicity we will assume that κ is constant across the cloud so that all the variability is due to the cloud density ρ . In the following, it will be convenient to nondimensionalize κ by the system size in the same way as the distances are nondimensionalized. Since we have taken $\langle \rho \rangle = 1$, κ is equal to the number of mean free paths across the unit cloud.

We can also define the optical path length:

$$\tau(x) = \kappa \int_{\text{path}} \rho(\vec{r}) dr \tag{10}$$

where the integration is over the straight line photon path of nondimensional distance x (x is the fraction of the cloud in the above optical path integral). The probability that a photon will travel a distance x without scattering is then given by the transmission function,

$$T = e^{-\tau}, \tag{11}$$

(known as “Beer’s Law”) and is the propagator from the radiative transfer equation. For “mean field” properties we require the statistical average of this quantity, the direct transmission $\langle T(x) \rangle$, (where for a fixed x , the average is to be taken over an ensemble of multifractal clouds).

In order to calculate the statistics of the random photon path distances x , the starting point is to write down an expression for the direct transmission averaged over the stochastic cloud variability:

$$\langle T(x) \rangle = \int_0^\infty e^{-\tau} p_\tau(\tau) d\tau, \tag{12}$$

where $p_\tau(\tau)$ is the probability density for finding an optical path length as given by Eq. (10) (see Ref. [60] for related stochastic media approaches).

We can then obtain the random distance probability density $p_x(x) = -\frac{\partial \langle T \rangle}{\partial x}$ and use this to obtain their statistical moments:

$$\langle x^{qp} \rangle = \int x^{qp} p_x(x) dx, \tag{13}$$

$p_x(x)$ is just the probability density for photon paths of physical length x (the subscript “ p ” on the exponent is for “photon”).

The random optical thickness τ is a one-dimensional integral over a large scale factor $\lambda \equiv 1/x$ of a multifractal field that has been developed to some fine inner scale with scale ratio Λ ; in other words, we start with an original multifractal with a high scale ratio $\Lambda \gg 1$ (i.e. small homogeneity scale = $1/\Lambda$) and spatially average to a larger distance $x = 1/\lambda$; $\lambda < \Lambda$. It is referred to as the “dressed field.” Mathematically, the dressed field $\rho_{\lambda,d}$ at scale ratio $\lambda < \Lambda$ is:

$$\rho_{\lambda,d} = \lambda \int_{1/\lambda} \rho_\Lambda(x') dx'. \tag{14}$$

For moments q below a critical value q_D , the bare and dressed statistics are the same to within factors of order unity: $\langle \rho_{\lambda,d}^q \rangle \approx \langle \rho_\Lambda^q \rangle$. However for $q > q_D$ the former diverge while the latter remain finite [57]. We assume here that $q < q_D$ so that it is an acceptable approximation to replace the dressed field by the bare field developed only down to the scale λ , i.e. we take $\rho_{\lambda,d} \approx \rho_\lambda$.

In the Monte Carlo approach to the problem, we consider that photons travel a distance x before scattering (determined by an exponential probability distribution of the optical thickness along the path). Since we assume the extinction coefficient (κ) is constant, over the distance x the optical thickness is:

$$\tau = \kappa \rho_{\lambda,d} x \approx \kappa \rho_\lambda \lambda^{-1} = \kappa \lambda^\gamma \tag{15}$$

where we have used the fact that for a multifractal field $\rho_\lambda = \lambda^\gamma$ with the singularities γ being an extremal Lévy random variable having probability density $p(\gamma)$, we find the following and we have made the approximation that the “bare” and “dressed” statistics are the same. This should be valid so long as x is small compared to 1 (the outer scale of the cloud): for small λ the bare field has undergone few cascade steps and therefore is less variable than the dressed field. In fact, the limit $\lambda \rightarrow 1$ is the uniform cloud, and thus serves as a useful check.

2.3. The direct transmission

We begin by finding an integral expression for $\langle T \rangle$ that can be evaluated. For technical reasons it is more convenient to use the normalization of the probability density so as to rewrite Eq. (12) as

$$\langle T(x) \rangle = 1 - \int_0^\infty (1 - e^{-\tau}) p_\tau(\tau) d\tau. \tag{16}$$

The problem now is that Lévy probability densities are not generally expressible in closed form except in the special cases $\alpha = 1$ (Cauchy probability density function), $\alpha = 1/2$ (“inverse Gaussian”), and $\alpha = 2$ (Gaussian). Nevertheless the Mellin transform of p_τ is straightforward so that with the help of the Parseval formula for products, we rewrite Eq. (16) in terms of the Mellin transformed quantities. We obtain an integral in the complex plane of the product of Mellin transforms (see, e.g. Bleistein [79]).

$$\langle T \rangle = 1 - \frac{1}{2\pi i} \int_{r-i\infty}^{r+i\infty} M[1 - e^{-\tau}; -q] M[p_\tau; 1 + q] dq \tag{17}$$

with the Mellin transform and its inverse given by:

$$M[f(\tau); q] \equiv \int_0^\infty \tau^{q-1} f(\tau) d\tau$$

$$f(\tau) = \frac{1}{2\pi i} \int_{r-i\infty}^{r+i\infty} \tau^{-q} M[f; q] dq. \tag{18}$$

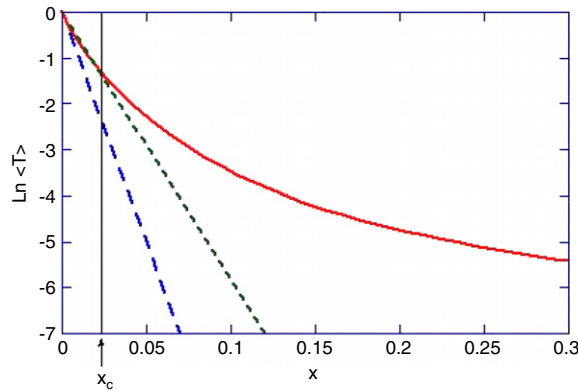


Fig. 2. $\ln\langle T \rangle$ vs. x (numerical integration), here for $k = 100$. The corresponding uniform transmission is shown as a dashed blue line, the dashed green line is the prediction of the “renormalized” medium approximation using K_{eff} developed below. For path lengths less than a critical x_c , the mean transmission is essentially exponential with this “effective” extinction coefficient at some reduced value. (For interpretation of the references to colour in this figure legend, the reader is referred to the web version of this article.)

The two Mellin transforms in Eq. (17) can be evaluated:

$$\begin{aligned} M[1 - e^{-\tau}; -q] &= -\Gamma(-q) \\ M[p_\tau(\tau); 1 + q] &= \kappa^q x^{q-K(q)}. \end{aligned} \tag{19}$$

The first transform is a standard result, where Γ is the gamma function. The second arises from the definition of the moment scaling function $K(q)$ (Eq. (9) combined with Eq. (13) with $x = \lambda^{-1}$). We therefore arrive at an essential expression,

$$\langle T(x) \rangle = 1 + \frac{1}{2\pi i} \int_{\substack{r-i\infty \\ 0 < r < 1}}^{r+i\infty} \kappa^q x^{q-K(q)} \Gamma(-q) dq. \tag{20}$$

The integration is along a vertical path which lies in the common strip of analyticity of the two Mellin transforms (see Fig. 9). While this does not at first seem like a simplification, it will provide a useful tool in finding asymptotic expansions for the photon path moments. Moreover it can be easily integrated numerically, as shown in Fig. 2.

Two observations are in order. The first is that the direct transmission through a cloud with a large variability in optical density can be much greater than for a uniform cloud of the same κ . The second is that there are at least two main regimes: a short-distance regime in which the transmission is approximately exponential at some reduced “renormalized” value of κ , and a long-distance regime in which the transmission falls off more gradually.

2.4. The singularity formalism for single scattering

We have seen that in multifractals developed over a large scale ratio λ , the probability and moment descriptions are simply related through a Legendre transformation (Eq. (6)). Lovejoy et al. [34] showed that for large κ an analogous set of exponents and relations exist for the radiative transfer. First, rather than consider the statistics of the photon path x , it will be convenient to define the distance normalized by the mean scattering distance κ^{-1} in a homogeneous cloud:

$$\tau_p = x\kappa \tag{20a}$$

and introduce the (random) “scattering singularity” γ_p for the random optical distance traversed by a photon before scattering:

$$\tau_p = \kappa^{\gamma_p}. \tag{21}$$

Unlike γ which is a real order of singularity of the cloud density field in real space, γ_p is simply the analogous exponent of the photon distances with respect to the extinction coefficient.

Now, we interpret the mean transmittance $\langle T \rangle$ averaged over the cloud statistics as the probability distribution of the random photon scattering distances:

$$\langle T \rangle = \Pr(\tau_p > \kappa^{\gamma_p}) \sim \kappa^{-c_p(\gamma_p)} \tag{22}$$

where we have anticipated that to leading order, the asymptotic expansion (large κ) for $\langle T \rangle$ is of the exponential form indicated and $c_p(\gamma_p)$ is the corresponding exponent (written in analogy to $c(\gamma)$, Eq. (5)). We now use (c.f. Eq. (20a)),

$$x = \tau_p/\kappa = \kappa^{\gamma_p-1} \tag{23}$$

and insert this into Eq. (20):

$$\kappa^{-c_p(\gamma_p)} = 1 + \frac{1}{2\pi i} \int_{\substack{r-i\infty \\ 0 < r < 1}}^{r+i\infty} \kappa^{q\gamma_p - K(q)(\gamma_p-1)} \Gamma(-q) dq. \quad (24)$$

If we now assume that $K(q)$ is analytic at the origin, we can take r to the left (past the pole in $\Gamma(-q)$ at the origin); this residue contributes a value -1 which cancels the 1 in Eq. (24) to yield

$$\kappa^{-c_p(\gamma_p)} = \frac{1}{2\pi i} \int_{r-i\infty}^{r+i\infty} \kappa^{q\gamma_p - K(q)(\gamma_p-1)} \Gamma(-q) dq. \quad (25)$$

Note that the assumption of analyticity at the origin is valid for many popular multifractal models such as the log-Poisson model [80] or the “ p model” [81] but is invalid for all the universal multifractals except the special “lognormal” multifractal $\alpha = 2$ (see Ref. [34] for the latter); the cases $\alpha < 2$ have a branch cut along the negative real axis ending at the origin. The final step is to make a transformation of variables and define the photon moment exponent $K_p(q_p)$,

$$\begin{aligned} q_p &= K(q) - q \\ K_p(q_p) &= K(q) \end{aligned} \quad (26)$$

to obtain:

$$\kappa^{-c_p(\gamma_p)} \sim \int_{-\infty}^{0-} \kappa^{-q_p\gamma_p + K_p(q_p)} f(q_p) dq_p \quad (27)$$

where we have deformed the limits of integration to lie on the negative q_p axis. The function f is an unimportant sub-exponential function [34]. If $K(q)$ and hence $K_p(q_p)$ have unique minima (recall, they are convex), and since $K(0) = K(1) = 0$, if $K(q)$ is real for $q < 0$, then this minimum occurs for real $q_p < 0$; it will lie on the domain of integration above. In that case, the “moving maximum” method of asymptotic approximation [82] allows us to conclude that for large enough κ :

$$\begin{aligned} c_p(\gamma_p) &= \max_q (q_p\gamma_p - K_p(q_p)) \\ K_p(q_p) &= \max_q (q_p\gamma_p - c_p(\gamma_p)) \end{aligned} \quad (28)$$

i.e. the same type of Legendre transform as for the multifractal cloud density statistics Eq. (6). This justifies the exponential form of $\langle T \rangle$ given in Eq. (21). The final formula relating cloud and scattering exponents follows by inverting the transform; we see for example that:

$$\langle \tau_p^{q_p} \rangle = \kappa^{K_p(q_p)} = \kappa^{q_p} \langle x^{q_p} \rangle. \quad (29)$$

The Legendre pairs in Eqs. (6) and (28) allow us to associate unique singularities with moments:

$$\begin{aligned} \gamma &= K'(q) = \frac{dq_p}{dq} + 1 \\ \gamma_p &= K'_p(q_p) = \frac{dq}{dq_p} + 1 \end{aligned} \quad (30)$$

from which we derive,

$$(\gamma - 1)(\gamma_p - 1) = 1; \quad c_p(\gamma_p) = \frac{c(\gamma)}{1 - \gamma}. \quad (31)$$

Eqs. (25), (27), (29) and (30) establish one to one relations between cloud densities and statistics, and photon paths and statistics; these will be quite helpful in interpreting the results below. These relationships between exponents are only between values which give dominant contributions to integrals; they are only exact in the limit $\kappa > \lambda \rightarrow \infty$). For example, using Eq. (31) we see that the most probable cloud density singularity, $\gamma_0 = -\frac{c_1}{\alpha-1}$, corresponds to the photon scattering singularity:

$$\gamma_{p0} = 1 - a(0); \quad a(0) = \frac{1}{1 - \gamma_0} = \left(1 + \frac{c_1}{\alpha - 1}\right)^{-1} \quad (32)$$

is the exponent for the photon distance x that will play a fundamental role in later developments. Since we saw γ_0 dominates the moment $q = 0$, and $q_p = K(q) - q$ we see that γ_{p0} gives the dominant contribution to $q_p = 0$, and finally, this shows

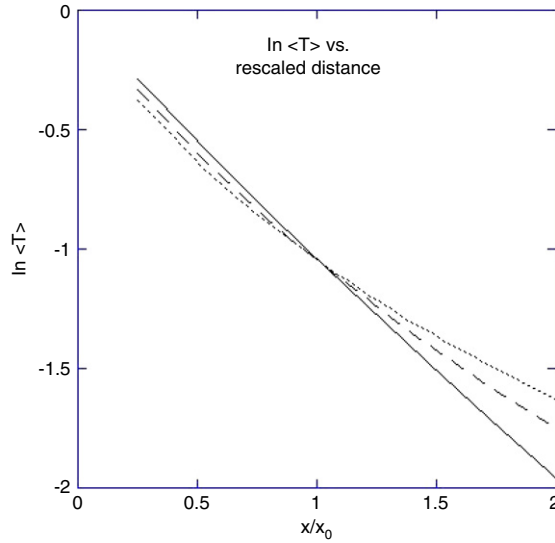


Fig. 3. $\ln\langle T \rangle$ vs. rescaled distance x/x_c (numerical integration). Solid line $\kappa = 10$, dashed line $\kappa = 100$, dotted line $\kappa = 1000$. Each curve intersects $\ln\langle T \rangle \approx -1$ near $\frac{x}{x_0} = 1$.

that $c'_p(\gamma_{p0}) = q_p(\gamma_{p0}) = 0$ so that γ_{p0} is in fact the most probable photon scattering singularity. In the case $\alpha = 2$, we easily obtain an analytic result [34]

$$c_p(\gamma_p) = \frac{(1 - (1 + C_1)(1 - \gamma_p))^2}{4C_1(1 - \gamma_p)} \tag{33}$$

$$K_p(q_p) = q_p - \frac{\sqrt{(1 + C_1)^2 + 4C_1q_p} - (1 + C_1)}{2C_1}.$$

In the following section, we show how this formalism can be extended to the case $1 < \alpha < 2$ and show the corresponding graphs of K_p, c_p .

3. Single scattering direct transmission and moments for $1 < \alpha < 2$

3.1. The transmission function

The idea of two scattering regimes is clearly manifest in the behavior of the transmission. For the special value of photon path length x_0 (corresponding to the most probable path length singularity γ_{p0}):

$$x = x_0 = \kappa^{1-\gamma_{p0}} = \kappa^{-a(0)} = \kappa^{-\left(1 + \frac{C_1}{\alpha-1}\right)^{-1}} \tag{34}$$

which might be called the renormalized *scattering length*. Eq. (20) is practically stationary with respect to a change in κ (see Fig. 3).

This stationary behavior can be traced to the fact that the linear term in the exponent of the integrand of Eq. (19) vanishes at x_0 leaving,

$$\langle T(x_0) \rangle = 1 + \frac{1}{2\pi i} \int_{r-i\infty}^{r+i\infty} \kappa^{\gamma_{p0}q^\alpha} \Gamma(-q) dq \approx e^{-1}. \tag{35}$$

The simplification comes about by choosing an integration path with $r \approx 0$ so that $\kappa^{\gamma_{p0}q^\alpha} \approx 1$ over the range where the gamma function makes its major contribution. We then apply the inverse Mellin transform of Eq. (18) (this argument does not work for $\alpha < 1$). The approximation is borne out by the numerics in Fig. 3. Since the transmission function falls to $1/e$ at x_0 it is easy to see that a good approximation for the transmission in the short distance regime is given by

$$\langle T \rangle \approx e^{-\kappa_{eff}x}, \quad x < x_0;$$

$$\kappa_{eff} = x_0^{-1} = \kappa^{a(0)} = \kappa^{\left(1 + \frac{C_1}{\alpha-1}\right)^{-1}}. \tag{36}$$

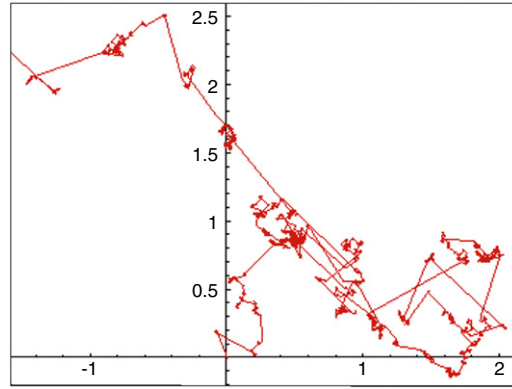


Fig. 4. This shows part of a random photon path using the derived distribution assuming each step is statistically independent ($\kappa = 1000$). Although the walk appears very similar to a Lévy flight (notice the clusters within clusters), the variance is in fact finite, the walk with independent steps will eventually tend to the standard gaussian brownian motion limit. The clustering is in fact due to the sharp difference in the statistics of short and long steps ($x < x_0$, $x > x_0$ respectively). In Section 4 we see that even for a large numbers of steps, they are not independent due to the long range correlations in the multifractal cloud (Fig. 5).

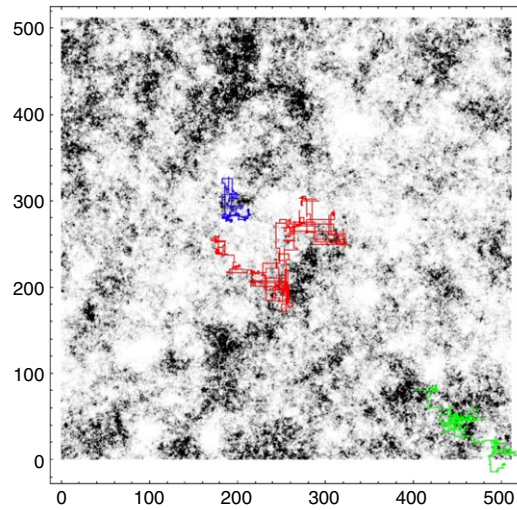


Fig. 5. Three photons paths, 100 scatters each on a conservative multifractal cloud (2-D), with $\alpha = 1.75$, $C_1 = 0.1$. We also see clustering when the photon moves into dense cloud regions. The cloud (and path) are periodic. Note here, discrete angle phase functions were used, isotropic in the four orthogonal directions.

The approximation of Eq. (36) is plotted in Fig. 2 and is a central result for non-extreme distances ($x < x_0$): for single scatterings the transmission is essentially exponential but with a reduced or renormalized extinction coefficient. More justification of this will be given later, Figs. 4 and 5 show the implications for photon path distributions. Another way of thinking about this is that $\langle T \rangle$ is determined almost entirely for short distances by the most probable singularity in the density field.

3.2. The photon moment statistics: the power law term

We turn our attention now to the path length moments,

$$\langle x^{q_p} \rangle = \int_0^1 x^{q_p} p_x(x) dx = - \int_0^1 x^{q_p} \frac{\partial \langle T \rangle}{\partial x} dx \quad (37)$$

(recall that the upper limit here is not infinity because the cloud has an outer scale of $x = 1$). Integrating by parts we get,

$$\langle x^{q_p} \rangle = -x^{q_p} \langle T \rangle \Big|_0^1 + \int_0^1 q_p x^{q_p-1} \langle T \rangle dx. \quad (38)$$

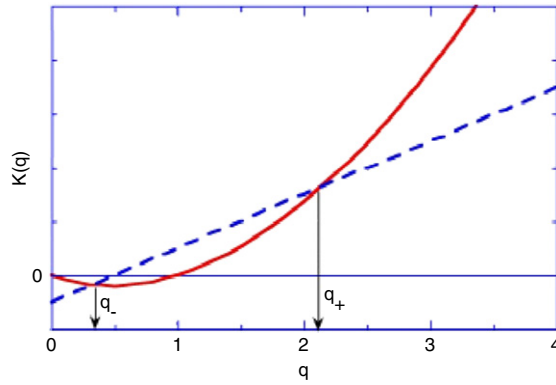


Fig. 6. $K(q)$ vs. q . The location of the poles in the integrand of Eq. (40) are given by the solution of $q_p + q = K(q)$.

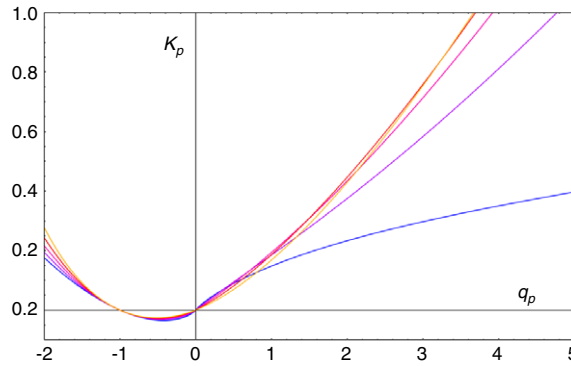


Fig. 7. $K_p(q_p)$ as a function of q_p obtained numerically using Eq. (26); all curves have $C_1 = 0.1$, from bottom to top, $\alpha = 1.1$ to 1.9 in steps of 0.2. Curves for other C_1 values are obtained using the fact that $K(q)/C_1 = K_p(q_p)/C_1$ is independent of C_1 .

The boundary term evaluates to $e^{-\kappa}$; it can be ignored for large κ . After substituting our integral expression for $\langle T \rangle$ we arrive at,

$$\langle x^{q_p} \rangle = 1 - e^{-\kappa} + W(q_p)$$

$$W(q_p) \equiv \frac{q_p}{2\pi i} \int_0^1 x^{q_p-1} \int_{\substack{r-i\infty \\ 0 < r < 1}}^{r+i\infty} \kappa^q x^{q-K(q)} \Gamma(-q) dq dx. \tag{39}$$

The order of integration may be reversed, justified on grounds of uniform convergence. The integral with respect to x is elementary, giving:

$$W(q_p) = \frac{q_p}{2\pi i} \int_{\substack{r-i\infty \\ 0 < r < 1}}^{r+i\infty} \frac{\kappa^q \Gamma(-q)}{q_p + q - K(q)} dq. \tag{40}$$

An analysis of Eq. (40) depends critically on the properties of the moment scaling function $K(q)$, which determines the locations of the poles of the integrand. For conservative multifractals, $K(q)$ is a convex function with $K(0) = K(1) = 0$ as shown in Fig. 6.

It is obvious from the figure that there will always be one real root of

$$q_p + q = K(q) \tag{41}$$

within $0 \leq q_- < 1$ for $-1 < q_p \leq 0$ so that the condition on the integration path in Eq. (40) can be satisfied by taking $q_- < r < 1$. We also see that the condition can never be satisfied for $q_p \leq -1$; in other words, these photon path moments diverge. If $K(q)$ is analytic (as is shown in the figure), then the positive moments can be handled with no modification. When $K(q)$ is given by Eq. (4) with $\alpha < 2$, however, $K(q)$ has a branch cut along the negative q -axis, and q_- will be complex and multiple-valued. In any event, so long as $-1 \leq q_p$ Eq. (40) is applicable.

It is important to appreciate that although Eq. (41) relating q , q_p , and $K(q)$ is the same as that obtained for analytic $K(q)$ relating dominant exponents, here, the relation determines the positions of poles in a complex integral. In this way, the relation continues to be important even when the exponential is not dominant (as we shall see for $1 < \alpha < 2$ below). See Figs. 7 and 8.

When $K(q)$ is analytic, the evaluation of Eq. (40) is straightforward, especially if the two roots can be obtained in closed form. The case for $\alpha = 2$ is given in Eq. (33).

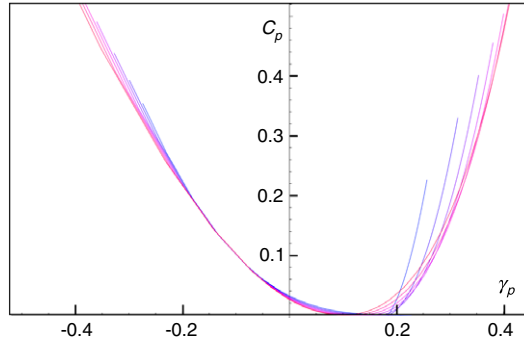


Fig. 8. $c_p(\gamma_p)$: Obtained by numerical Legendre transformation of the above. Here we show $\alpha = 1.3$ to 1.9 (bottom to top, in steps of 0.1).

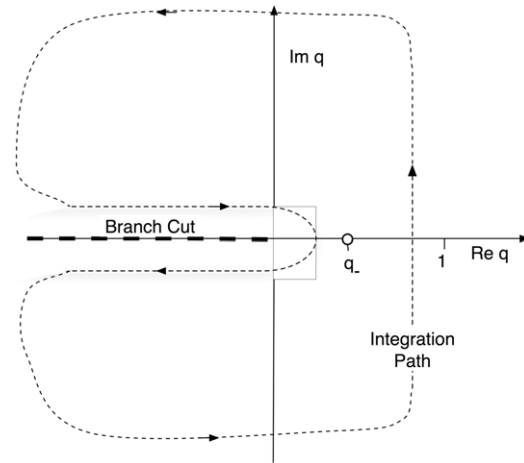


Fig. 9. The integration path for the integral in Eq. (40).

3.3. The photon moment statistics: The logarithmic terms

We have seen that the poles will give us power law terms. Let us now proceed to a complete analysis of the integral in Eq. (40). First consider the case of negative moments when $-1 < q_p \leq 0$. Our strategy (see Fig. 9) is to displace the contour of integration as far as possible to the left: in so doing we pick up the contribution from the residue of the pole at q_- and are left with the contribution from the hair-pin path along the branch cut and a vanishing contribution from the path at $\text{Re}(q) \rightarrow -\infty$.

Using Cauchy’s Residue Theorem, Eq. (40) evaluates to:

$$W(q_p) = \frac{q_p \Gamma(-q_-)}{1 - K'(q_-)} \kappa^{q_-} + \frac{q_p}{2\pi i} \int_{-\infty}^{0+} \frac{\kappa^q \Gamma(-q)}{q_p + q - K(q)} dq. \tag{42}$$

The right hand side integral is evaluated along the hairpin path by using Watson’s lemma for loop integrals which provides an asymptotic expansion in κ . We omit the details and refer the reader to the treatment in Olver [83]. There is a trivial contribution of -1 in the expansion due to the pole in $\Gamma(-q)$ at the origin, which cancels the $+1$ term in Eq. (35). When the next two leading terms in q_p are evaluated, we get (ignoring the $e^{-\kappa}$ boundary term):

For $q_p < 0$,

$$\begin{aligned} \langle x^{q_p} \rangle &\sim A \kappa^{q(q_p)} + B (\log \kappa)^{-\alpha} + C (\log \kappa)^{-(\alpha+1)} + \dots \\ A &= \frac{q_p \Gamma(-q(q_p))}{1 - K'(q(q_p))} \\ B &= \frac{C_1}{q_p \Gamma(2 - \alpha)} \end{aligned}$$

$$C = \left(\frac{\gamma_E \gamma_0}{q_p} - \frac{2\gamma_0(1 - \gamma_0)}{q_p^2} \right) \frac{1}{\Gamma(-\alpha)}, \quad \gamma_0 = \frac{-C_1}{\alpha - 1}. \quad (43)$$

(where $\gamma_E = 0.57 \dots$ is the Euler gamma).

Note that the two logarithmic terms vanish for $\alpha = 2$ as they must do if the branch cut goes away. For large κ it is the first (algebraic) term which dominates the negative moments since $q(q_p)$ is positive. It is also important to remember that $q(q_p)$ is a function of q_p determined by the solution of Eq. (41).

The analysis for the moments $q_p > 0$ is not as straightforward because q_- is replaced by multiple complex roots. They contribute a term that goes as $\kappa^{-|f(q_p)|}$. For large κ (or large enough q_p) this is not a concern and the leading terms in the asymptotic expansion are the logarithmic terms in Eq. (43). In other words, the above formula is also valid for $q_p > 0$. In this case, we see that for large enough κ , the log terms are dominant with respect to the power law terms. However numerically we find that for $q_p \geq 1$ and $1 < \alpha < 2, 0 < C_1 < 1$ they are generally subdominant until $\kappa > 100$.

Since for values of κ having practical interest ($\kappa < 500$ i.e. clouds with mean optical thickness < 500), the power law term is important, it is necessary to find an approximation for the complex root $q(q_p)$:

$$q \approx - \left(1 + \frac{C_1}{\alpha - 1} \right)^{-1} q_p + e^{\pm i\pi\alpha} \left(\frac{C_1}{\alpha - 1} \right) \left(1 + \frac{C_1}{\alpha - 1} \right)^{-1-\alpha} q_p^\alpha; \quad q_p > 0. \quad (44)$$

We can also define the exponent $a(q_p)$:

$$a(q_p) = a(0) = \left(1 + \frac{C_1}{\alpha - 1} \right)^{-1}; \quad q_p \leq 0$$

$$a(q_p) = - \frac{\text{Re}(q(q_p))}{q_p} \approx a(0) - \cos(\pi\alpha) \left(\frac{C_1}{\alpha - 1} \right) a(0)^{-1-\alpha} q_p^\alpha; \quad q_p > 0. \quad (45)$$

For many purposes, it is sufficient to take $a(q_p) \approx a(0)$. Using this result and the properties of the gamma function, becomes for $q_p > 0$:

$$\langle \chi^{q_p} \rangle \sim \Gamma(1 + a(0) q_p) \kappa^{-a(0)q_p} + B(\log \kappa)^{-\alpha} + C(\log \kappa)^{-(\alpha+1)} + \dots \quad (46)$$

with B, C given in Eq. (42). We see that if κ is small enough so that we neglect the log κ corrections, that:

$$\langle \chi^{q_p} \rangle \approx \kappa_{\text{eff}}^{-q_p}; \quad \kappa_{\text{eff}} = \kappa^{a(q_p)}. \quad (47)$$

Since a homogeneous cloud has $\langle \chi^{q_p} \rangle = \kappa^{-q_p}$ we see that if $a(q_p) \approx a(0)$ that the photon statistics are the same as for a homogeneous cloud with $\kappa^{a(0)}$ in place of κ ; a is thus a “renormalization” exponent.

In fact, this expression will be applicable to both positive and negative moments, the only distinction being that (for very large κ) the algebraic and logarithmic terms trade places in importance as q_p changes sign. Once again, we have seen that the statistics of short pathlengths (which are described by the negative q_p) differ from the long pathlength (described by the positive q_p). This is not really surprising since the Lévy probability density for the density singularities is “maximally asymmetric” (between positive and negative values), the exception being the symmetric Gaussian case ($\alpha = 2$). But for this exception there is no branch cut: the logarithmic terms vanish so the moment function is always algebraic, a result that one obtains whenever $K(q)$ is analytic. Fig. 10 shows that the above approximations are indeed quite accurate for $q_p = 2$.

4. Conclusion

In terrestrial and astrophysical systems, radiation typically is transported through highly heterogeneous media. Indeed, if we consider turbulence in the broad sense, i.e. including astrophysical MHD turbulence, and in terrestrial atmospheres, multiphase – water/air – and other effects, then radiative transfer applications typically involve turbulent systems (e.g. “clouds”). In the last 25 years it has become increasingly clear that both astrophysical and atmospheric turbulent “clouds” are highly heterogeneous multifractals with interesting, nontrivial, wide range scaling properties ranging over many decades in scale. Unfortunately, with relatively few exceptions, radiative transfer theory has been restricted to plane parallel (or spherically symmetric) geometries wherein horizontal heterogeneity is ignored. The main exceptions to this are purely numerical studies of “3D radiative transfer”, typically with relatively thin optical thicknesses so that the effects of heterogeneity are not large. At the same time, the occasional analytic approaches to the problem have been mostly restricted to fairly academic problems such as deterministic monofractal clouds, or to conservative multifractals, or to single scattering.

In this paper, we return to the problem of optically thick, highly heterogeneous multifractal clouds, and extend the early work in a number of ways, ultimately developing a theoretical framework which applies to realistic cloud variability. In this first of two papers, we showed how our earlier single scattering theory valid for conservative fields (those which are the direct outcome of multiplicative cascade processes), can be extended from clouds with analytic scaling exponents (such as “lognormal” multifractals), to clouds with exponents non-analytic at the origin (“Log-Lévy” multifractals). While this may

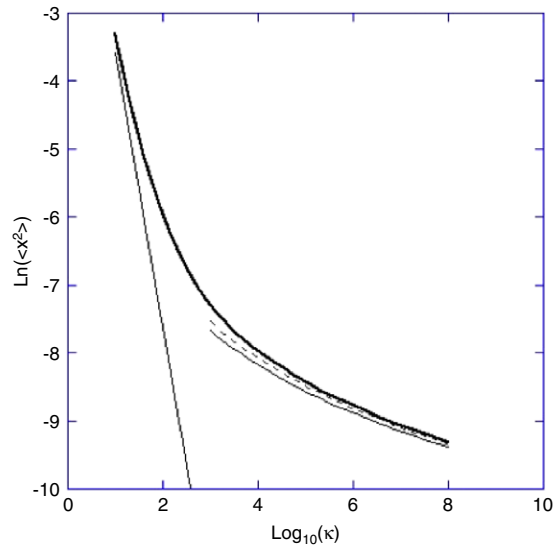


Fig. 10. For $\alpha = 1.75$, $C_1 = 0.1$, we show $\ln\langle x_2 \rangle$ versus $\log_{10} k$. The heavy solid line gives the numerical integration of Eq. (39). The thin solid lines indicate the first term (exponential) and second (logarithmic) terms respectively of Eq. (46). The dashed line shows the improvement when the third term of Eq. (46) is included.

appear technical, physically it corresponds to clouds which are dominated by “Lévy holes”, i.e. possibly large and frequently occurring low density regions which are obviously important for the transfer. By developing asymptotic expansions for single scattering cloud statistics in thick clouds, we show how these holes give increased transmission with qualitatively new (log transmission) behavior while retaining power law terms. We develop an exponent formalism which relates the single scattering photon exponents to the cloud statistical exponents, showing that except for very thick clouds, this power law dominates. Therefore to a first approximation (small κ), this enables us to “renormalize” the cloud so that the mean cloud transmission is approximately the same as a plane parallel cloud with optical thick thickness $\kappa_{eff} = \kappa^a$; we calculate the exponent a theoretically from the cloud statistics (since we considered clouds of unit length with mean nondimensional density = 1, the nondimensional extinction coefficient κ is equal to the mean cloud optical thickness). However two effects cause deviations from this power law renormalization. First, for thick enough clouds the “Lévy hole” power law corrections mentioned above mean that single scattering is ultimately dominated by the holes and so the power law renormalization underestimates the thick cloud single scatter transmission.

Second, the total transmission involves multiple scattering. This is the subject of a subsequent paper in which we will quantify the effect of multiple scattering with the help of numerical simulations, showing that the N scattering statistics in a cloud is very nearly given by the theoretical single scattering statistics but for a much thinner cloud: $x_N(\kappa) \approx x_1(N^{-1/2}\kappa)$ and allowing these “renormalized” single scattering results to be used as approximations to multiple scattering. We also extend these results to the more realistic case of nonconservative clouds, i.e. those modeled by fractionally integrated turbulent cascades. In this case, we use numerical methods to show that this single scattering renormalization was still approximately valid even for thick clouds.

The results in this paper provide for the first time theoretical results applicable to realistic optically thick multifractal clouds. This may have important consequences for estimates of cloud liquid water from satellite observations, and for the handling of radiation in numerical climate models or numerical models of stellar atmospheres.

Acknowledgements

This research was carried out for scientific purposes only, it received no specific funding. We thank P. Gabriel for detailed comments on early drafts of this paper, and we thank A. Davis for useful discussions.

References

- [1] S. Lovejoy, D. Schertzer, V. Allaire, T. Bourgeois, S. King, J. Pinel, J. Stolle, *Geophys. Res. Lett.* 36 (2009) L01801, doi:10.1029/2008GL035863.
- [2] S. Lovejoy, D. Schertzer, J.D. Stanway, *Phys. Rev. Lett.* 86 (2001) 5200.
- [3] S. Lovejoy, D. Schertzer, *J. Hydrol.* (2006) doi:10.1016/j.hydrol.2005.02.042.
- [4] A.N. Witt, K.D. Gordon, *Astrophys. J.* 463 (1996) 681.
- [5] F. Varosi, E. Dwek, in: W.H. Waller, et al. (Eds.), *The Ultraviolet Universe at Low and High Redshift: Probing the Progress of Galaxy Evolution*: College Park MD May 1997, AIP, College Park, MD, 1997.
- [6] M. Juvela, *Astron. Astrophys.* 322 (1997) 943.
- [7] A.N. Witt, K.D. Gordon, *Astrophys. J.* 528 (2000) 799.

- [8] A. Acker, K. Gesicki, Y. Grosdidier, S. Durand, *Astron. Astrophys.* 384 (2002) 620.
- [9] Y. Grosdidier, A. Acker, in: P.S.a.J.-P.Z.M. Heydari-Malayeri (Ed.), *Evolution of Massive Stars, Mass Loss and Winds*, in: EAS Publications Series, vol. 13, Aussois and Oléron, France, 2004, p. 317.
- [10] D. Bazell, F.X. Désert, *Astrophys. J.* 333 (1988) 353.
- [11] M. Beech, *Astrophys. Space Sci.* 192 (1992) 103.
- [12] S. Blacher, J. Perdang, *Vistas Astron.* 33 (1990) 393.
- [13] A.G. Gill, R.H. Henriksen, *Astrophys. J.* 365 (1990) L27.
- [14] E. Falgarone, T.G. Phillips, C.K. Walker, *Astrophys. J.* 378 (1991) 186.
- [15] M.S. Miesch, J. Bally, *Astrophys. J.* 429 (1994) 645.
- [16] C.M. Brunt, M.H. Heyer, *Astrophys. J.* 566 (2002) 289.
- [17] E. Falgarone, P. Hily-Blant, F. Levrier, *Astrophys. Space Sci.* 292 (2004) 89.
- [18] D. Schertzer, S. Lovejoy, *Physico-Chemical Hydrodyn.* 6 (1985) 623.
- [19] M. Lilley, S. Lovejoy, K. Strawbridge, et al., *Phys. Rev. E* 70 (2004) 036307.
- [20] S. Lovejoy, D. Schertzer, M. Lilley, K. Strawbridge, A. Radkevitch, Q. J. R. Meteorol. Soc. 134 (2008) 277.
- [21] M. Lilley, S. Lovejoy, K. Strawbridge, D. Schertzer, A. Radkevitch, Q. J. R. Meteorol. Soc. 134 (2008) 301.
- [22] A. Radkevich, S. Lovejoy, K. Strawbridge, D. Schertzer, M. Lilley, Q. J. R. Meteorol. Soc. 134 (2008) 316.
- [23] A. Radkevich, S. Lovejoy, K. Strawbridge, D. Schertzer, *Physica A* 382 (2007) 597.
- [24] S. Lovejoy, S. Hovde, A. Tuck, D. Schertzer, *Geophys. Res. Lett.* 35 (2008) L01802.
- [25] S. Lovejoy, A.F. Tuck, S.J. Hovde, D. Schertzer, *J. Geophys. Res.* 114 (2009) D07111, doi:10.1029/2008JD010651.
- [26] S. Lovejoy, P. Gabriel, A. Davis, et al., *J. Geophys. Res.* 95 (1990) 11699.
- [27] P. Gabriel, S. Lovejoy, A. Davis, et al., *J. Geophys. Res.* 95 (1990) 11717.
- [28] A. Davis, S. Lovejoy, P. Gabriel, et al., *J. Geophys. Res.* 95 (1990) 11729.
- [29] P. Meakin, *J. Phys. A* 20 (1987) L771.
- [30] S. Lovejoy, D. Schertzer, P. Silas, *Water Resour. Res.* 34 (1998) 3283.
- [31] H. Weissman, S. Havlin, *Phys. Rev. B* 37 (1988) 5994.
- [32] S. Lovejoy, D. Schertzer, B. Watson, in: S. Keevallik, O. Kärner (Eds.), *I.R.S. 92*, 1993, p. 108.
- [33] C. Marguerite, D. Schertzer, F. Schmitt, et al., *J. Marine Systems* 16 (1–2) (1998) 69.
- [34] S. Lovejoy, W. B. S. D., et al., in: L. Briggs (Ed.), *Particle Transport in Stochastic Media*, vol. 1, American Nuclear Society, Portland, Or, 1995, p. 750.
- [35] S. Havlin, D. Ben-Avraham, *Adv. Phys.* 36 (1987) 695.
- [36] J.P. Bouchaud, A. Georges, *Phys. Rep.* 195 (1990) 127.
- [37] S. Chandrasekhar, *Radiative Transfer*, Clarendon Press, Oxford, 1950.
- [38] V.P. Busygina, N.A. Yevstatov, E.M. Feigelson, *Izv. Acad. Sci. USSR Atmos. Oceanic Phys.* 9 (1973) 1142.
- [39] T. McKee, S.K. Cox, *J. Atmospheric Sci.* 33 (1976) 2014.
- [40] R.W. Preisendorfer, G.I. Stephens, *J. Atmospheric Sci.* 41 (1984) 709.
- [41] J.A. Weinman, P.N. Swartzrauber, *J. Atmospheric Sci.* 25 (1968) 497.
- [42] R.M. Welch, S. Cox, J. Davis, *Solar Radiation and Clouds* (1980).
- [43] P.M. Gabriel, S.-C. Tsay, G.L. Stephens, *J. Atmospheric Sci.* 50 (1993) 3125.
- [44] R.F. Cahalan, L. Oreopoulos, A. Marshak, et al., *Bull. Am. Meteorol. Soc.* 86 (2005) 1275.
- [45] D.B. Mechem, Y.L. Kogan, M. Ovtchinnikov, A.B. Davis, R.R. Cahalan, E.E. Takara, R.G. Ellingson, 12th ARM Science Team Meeting Proceedings, St. Petersburg, Florida, 2002, p. 1.
- [46] N.a.H.I. Ferlay, *J. Atmospheric. Sci.* 63 (2006) 1200.
- [47] N. Ferlay, Harumi Isaka, Philip Gabriel, Albert Benassi, *J. Atmospheric. Sci.* 63 (2006) 1213.
- [48] A. Marshak, A.B. Davis, *Physics of Earth and Space Environments*, Springer, 2005, p. 686.
- [49] P. Gabriel, S. Lovejoy, D. Schertzer, G.L. Austin, 6th Conference on Atmospheric Radiation, Amer. Meteor. Soc, Boston, Williamsburg, Va, 1986, p. 230.
- [50] R.F. Cahalan, in: A. Deepak, H. Flemming, J. Theon (Eds.), *Advances in Remote Sensing Retrieval Methods*, A. Deepak, Hampton Va, 1989.
- [51] S. Lovejoy, D. Schertzer, in: J.F.G.C. Lenoble (Ed.), *Inter. Rad. Symp.* 88, Deepak, 1989, p. 99.
- [52] H.W. Barker, J.A. Davies, *Remote Sens. Environ.* 42 (1992) 51.
- [53] R.F. Cahalan, W. Ridgeway, W.J. Wiscoombe, et al., *J. Atmospheric Sci.* 51 (1994) 2434.
- [54] R. Cahalan, *Nonlinear Proc. Geophys.* 1 (1994) 156.
- [55] P. Gabriel, S. Lovejoy, D. Schertzer, et al., *Geophys. Res. Lett.* 15 (1988) 1373.
- [56] S. Lovejoy, D. Schertzer, *J. Geophys. Res.* 95 (1990) 2021.
- [57] D. Schertzer, S. Lovejoy, *J. Geophys. Res.* 92 (1987) 9693.
- [58] A. Marshak, A.B. Davis, in: A. Marshak, A.B. Davis (Eds.), *3D Radiative Transfer in Cloudy Atmospheres*, 2005, p. 653.
- [59] A.B. Davis, A. Marshak, K.P. Pfeilsticker, Ninth ARM Science Team meeting, US Dept. of Energy, San Antonio Texas, March 22–26, 1999, p. 1.
- [60] K.F. Evans, *Geophys. Res. Lett.* 20 (1993) 2075.
- [61] K.M. Gierens, *Beitr. Phys. Atmos.* 66 (1993) 73.
- [62] K.M. Gierens, *Beitr. Phys. Atmos.* 69 (1996) 355.
- [63] K.M. Gierens, *J. Atmospheric Sci.* 53 (1996) 3333.
- [64] R. Borde, H. Isaka, *J. Geophys. Res.* 101 (1996) 29.
- [65] A. Davis, S. Lovejoy, D. Schertzer, *SPIE* 1558 (1991) 37.
- [66] A. Davis, S. Lovejoy, D. Schertzer, in: S. Keevallik, O. Kärner (Eds.), *International Radiation Symposium 92*, Deepak, Hampton, Virginia, 1993, p. 112.
- [67] C. Naud, D. Schertzer, S. Lovejoy, in: W. Woyczynski, S. Molchanov (Eds.), *Stochastic Models in Geosystems*, Springer-Verlag, New York, 1996, p. 239.
- [68] D. Schertzer, S. Lovejoy, F. Schmitt, et al., *Fractals* 5 (1997) 427.
- [69] Y. Tessier, S. Lovejoy, D. Schertzer, *J. Appl. Meteorol.* 32 (1993) 223.
- [70] D. Sachs, S. Lovejoy, D. Schertzer, *Fractals* 10 (2002) 253.
- [71] S. Corrsin, *J. Appl. Phys.* 22 (1951) 469.
- [72] A. Obukhov, *Izv. Akad. Nauk. SSSR. Ser. Geogr. I Geofiz* 13 (1949) 55.
- [73] S. Lovejoy, D. Schertzer, in: G. Wilkinson (Ed.), *Fractals in Geoscience and Remote Sensing*, Office for Official Publications of the European Communities, Luxembourg, 1995, p. 102.
- [74] D. Schertzer, S. Lovejoy, *Physica A* 185 (1992) 187.
- [75] G. Parisi, U. Frisch, in: M. Ghil, R. Benzi, G. Parisi (Eds.), *Turbulence and Predictability in Geophysical Fluid Dynamics and Climate Dynamics*, North Holland, Amsterdam, 1985, p. 84.
- [76] S. Lovejoy, D. Schertzer, *J. Hydrol.* 322 (2006) 59.
- [77] T.C. Halsey, M.H. Jensen, L.P. Kadanoff, et al., *Phys. Rev. A* 33 (1986) 1141.
- [78] J.W. Kantelhardt, et al., *Physica A* 316 (2002) 87.
- [79] N. Bleistein, R.A. Handelsman, *Asymptotic Expansions of Integrals*, Dover, Mineola, 1986.
- [80] Z. She, S. E. Levesque, *Phys. Rev. Lett.* 72 (1994) 336.
- [81] C. Meneveau, K.R. Sreenivasan, *Phys. Rev. Lett.* 59 (1987) 1424.
- [82] C.M. Bender, S.A. Orszag, *Advanced Mathematical Methods for Scientists and Engineers*, Mc Graw Hill, New-York, NY, 1978.
- [83] F.W.J. Olver, *Asymptotics and Special Functions*, Academic, New York, 1974.